Formation of iron sulfide photocatalytic colloidal dispersion via pulsed laser ablation in liquids

IOP Conf. Series: Materials Science and Engineering **613** (2019) 012034 doi:10.1088/1757-899X/613/1/012034

Formation of iron sulfide photocatalytic colloidal dispersion via pulsed laser ablation in liquids

Lukáš Vála[1], Veronika Vavruňková[1], Věra Jandová[2], Michal Pola[1], Tomáš Křenek[1]*

[1] University of West Bohemia, Research Centre New Technologies 30614 Pilsen, Czech Republic
[2] Institute of Chemical Process Fundamentals, Czech Academy of Sciences, Rozvojova 135, 160 00 Prague 6, Czech Republic

E-mail: tkrenek@ntc.zcu.cz

Abstract. Pulsed laser irradiation of iron sulfide in water and ethanol allows laser ablation and generation of FeS nano/micro particles. Measurement of the size distribution reveals 100, 1000 and 5000 nm sized particles in water and 180 nm sized particles in ethanol. The values of zeta potential: 13.2 mV for colloid in water confirm incipient stability and tendency for coagulation whereas the value: -40.6 mV shows good stability of ablatively achieved nanoparticles in ethanol. SEM analyses of particles obtained by evaporation of solvents on Ta substrate revealed shapeless, roundshape and sheet-like morphology of agglomerates whose size span from units up to tens of μm. Also spherical particles sized around tens of nm were detected. EDX shows Fe/S ratio ~3.25 and ~ 1.2 for particles ablated in water and ethanol respectively. Raman spectroscopy indicates the formation of mackinawite ($Fe_{1+x}S$) and pyrrhotite ($Fe_{1-x}S$) phase. The photocatalytic effect of prepared water colloid was tested in methylene blue (MB) degradation under the daylight.

1. Introduction

Ferrous sulfide represents an attractive material for solar cell application [1] which exhibits also interesting semiconducting [2], magnetic [3] and biocatalytic [4] and photocatalytic [5] properties. Also, hydrogen evolution reaction (HER) electrocatalytic activity of ferrous sulfide has been confirmed [6]. Moreover, some iron sulfides such as mackinawite (FeS) and pyrite (FeS_2) have been considered as excellent materials for mercury adsorption due to their high affinity towards Hg^{2+} [eg.7] and for ability to capture also other toxic elements, including Cu, Cr, Cd, Pb, and As [8-11]. FeS offers abundance, non-toxicity and low price. The iron sulfide (FeS) belongs between considerably polymorphic compounds with complex phase diagram including seven phases: pyrite (cubic- FeS_2), marcasite (calcium chloride structure-FeS_2), pyrrhotite-IT ($Fe_{1-x}S$), pyrrhotite-4M (Fe_7S_8), Fe_9S_{10}, greigite (cubic spinel- Fe_3S_4), troilite-2H (FeS) and mackinawite ($Fe_{1-x}S$) [12-15]. Except stable pyrite (FeS_{2p}) and pyrrhotite phases are metastable or unstable. Pyrite phase of iron sulfide is suitable as an absorbing material for thin film solar cells because of its band gap (Eg = 0.95 eV) and high absorption coefficient (~105 cm^{-1}) [16].

FeS stoichiometric iron sulfide has troilite structure which possesses antiferromagnetic properties at room temperature. Above 120°C, troilite transforms to the NiAs-type structure composing of ($Fe_{1-x}S$) and Fe_7S_8 pyrrhotites [17]. Vacancies of Fe cause that many pyrrhotites ($Fe_{1-x}S$) create compositions with interesting magnetic and electrical properties [18, 19]. The non-stoichiometric $Fe_{1-x}S$ shows

different morphologies, including nanorods [20], whiskers [21], and U-shaped microslots [22]. Nanoparticles of iron sulfide have been obtained via high energy mechanical milling [23] and by hydrothermal methods [eg. 24]. Pulsed laser deposition of nanostructured FeS in the vacuum has been described in our recent studies [25, 26]. To best of our knowledge there is not published any information about LAL of iron sulfide. Laser ablation in liquid (LAL) has been developed into an important method to prepare metal, semiconductor, and even polymer colloidal dispersion of nanoparticles. As a technique, LAL is somewhat different from the other laser ablation approaches operate in vacuum or gaseous environments because the liquid medium not only provides some effective controlling parameters for fabrication, but also greatly affects the morphology and microstructure of the products [27].

Here we report the first study on LAL of iron sulfide. LAL of FeS results in generation of less stable colloid in water and good stable colloid in ethanol. The morphology of ablatively achieved particles is roundshape and sheet-like and Raman spectroscopy suggests formation of mackawite and pyrrhotite phase. Photocatalytic efficiency of the aqueous colloid for methylene blue (MB) degradation has been shown.

2. Experimental

A 3rd harmocnic of pulsed Nd:YAG laser with base wavelength 1064 nm (model Q SMART 850, wavelength: 355 nm , energy: 180 ± 5 mJ per pulse, pulse duration: 10 ns, repetition rate: 10 Hz, pulse full width at half maximum: 23 ns) was focused by lens (f = 15 cm) on the spot area of 0.02 cm^2 on FeS target. Simple tubular Pyrex reactor (70 mL in volume) reactor was furnished with a borosilicate glass windows and filled with DEI water or ethanol. The duration of irradiation was 2 hours.

The irradiated target of FeS pellet with diameter 8 mm and height 5 mm was positioned vertically in the center of the reactor. After the irradiation the prepared colloid was characterized by MALVERN Zetasizer for the measurement of the size of particles and Zeta potential of the colloid and part of colloid has been evaporated on Ta substrate in order to measure SEM-EDX and Raman spectroscopy of nanoparticles/agglomerates.

Size distribution of the particles in prepared colloids and its zeta potential were measured by Dynamic Light Scattering – Zetasizer Nano (Malvern).

A SEM (Scanning Electron Microscope, Tescan Indusem) with mounted EDS was used for the composition evaluation of the particles obtained by evaporation of the solvents of the colloids. Particles were catching on Ta substrate and analyzed by SEM and EDS at acceleration voltage 15 kV.

Raman spectra were obtained using a DXR Raman microscope with Diode-pumped solid state laser emitting at 532 nm using high resolution gratings working in the range of 50 – 1800 cm^{-1} and spectral resolution 2 cm^{-1} FWHM.

The FeS pellet was made at 100 atm. on a hydraulic press from a commercially available iron sulfide powder (FeS, 99% Fe, Aldrich).

The photocatalylic oxidation of MB by FeS nanoparticles dispersed in water was performed as follows: 1ml of 0.05mM solution of methylene blue and 2.5 ml of freshly prepared aqueous colloid. This mixture was exposed to daylight (without external light source) for 180 min. Intensity of the light was $\Phi \sim 800$ lm. The depletion of MB was measured each 30 minutes by UV spectrometer (RED TIDE USB650 UV).

3. Results and discussion

Highly focused pulsed irradiation of FeS target in water/ethanol results in generation of colloids based on FeS NPs/agglomerates. The color of solvents (DEI water, ethanol) changed into slightly brownish. The distribution of NPs and the progress of agglomeration were measured by Malvern Zetasizer analyzer. Fig. 1 A depicts size distribution of the particles obtained by LAL of FeS in DEI water were several fractions have been revealed. The size distribution around 100 nm, 1000 nm and 5000 nm has been detected. The measuring of size distribution depending on time shows slowly continuing agglomeration of the particles. The intensity of the peak which belongs to 100 nm sized particles decreases and the peaks attributed to 1000 and 5000 nm sized agglomerates become more intensive.

Zeta potential of the colloid measured immediately after irradiation represents value 13.2 mV which suggests incipient instability of the colloid. It corresponds with agglomeration process. The FeS particles generated via LAL in ethanol exhibit higher stability compared to water colloid. Fig. 1 B gives information about one size fraction varies around 180 nm where the values are not changing in dependence on time. Also, the value: -40.6 mV of zeta potential confirms good stability of the prepared colloid.

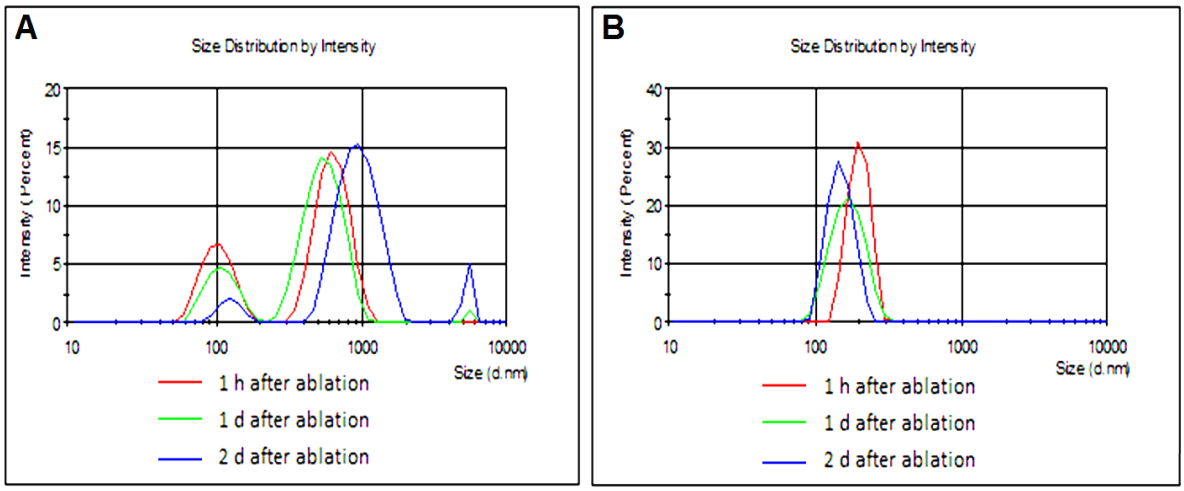

Fig. 1 Size distribution of particles generated in water (A) and in ethanol (B)

In order to search phase and chemical composition of prepared FeS particles the colloids were evaporated in small cuvette and achieved particles were deposited on Ta substrate. The SEM (Fig. 2) revealed shapeless, roundshape and needle-like/sheet-like morphology in case of colloid prepared by laser ablation in the water (Fig. 2 A). More detailed view shows also smaller spherical particles whose size varies around tens of nm. The particles obtained by evaporation of the ethanol exhibits shapeless agglomerates with sheet-like units with random orientation. Similar flower-like morphology was observed eg. in case of FeS nanosheets synthesized by a poly(vinyl alcohol)-assisted precipitation method [28] or after thermal decomposition of the organometallic precursor in oleylamine [29]. Also in case of ethanol colloid, spherical particles sized in order of tens of nm are present.

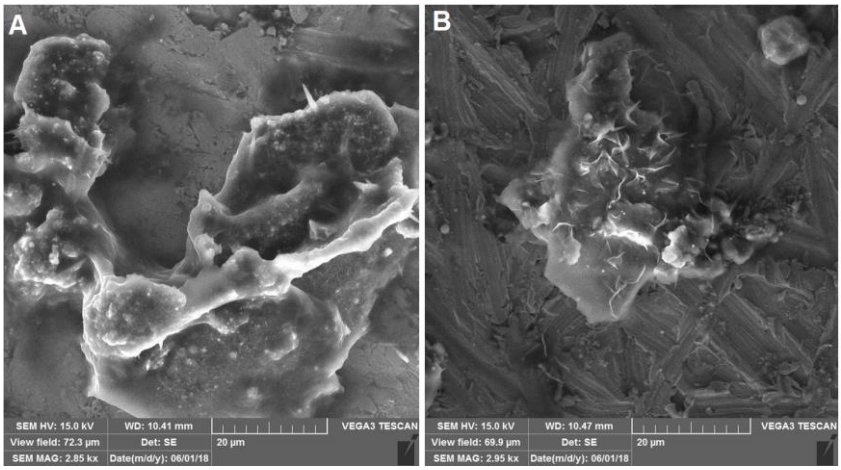

Fig. 2 SEM images of the FeS particles obtained after evaporation of water (A) and ethanol (B)

EDX analyses allow assessment of the chemical composition of the particles. The agglomerates achieved using LAL in water show Fe/S ratio of at.% around 3.25 and in ethanol Fe/S ratio ~ 1.2. These values of S-deficient objects indicate some decomposition of FeS during LAL. The decomposition is more significant in water environment where iron sulfide can undergo some hydrothermal processes [30].

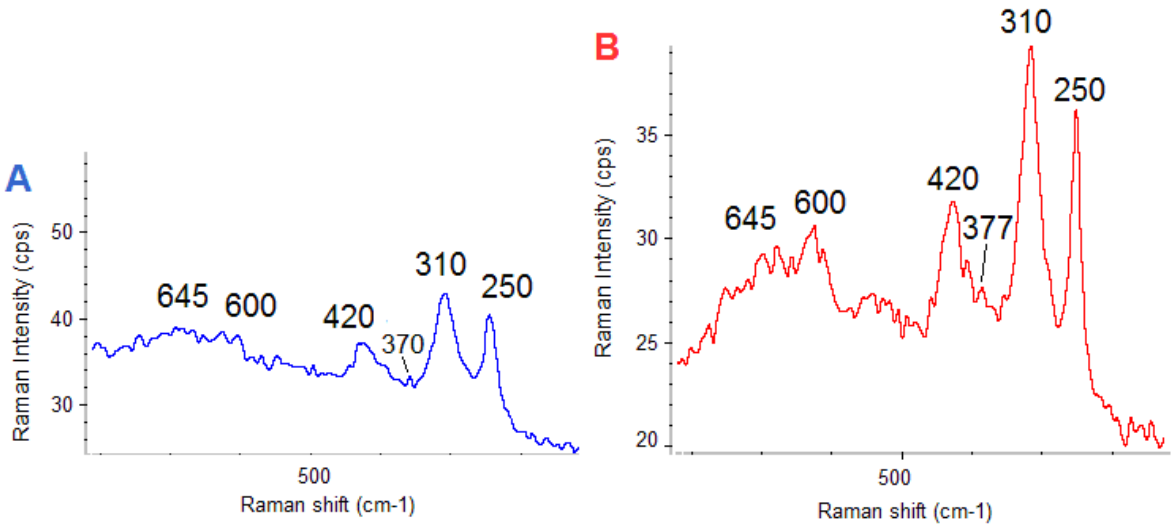

Fig. 3 Raman spectroscopy of FeS particles obtained by LAL of FeS target in water (A) and in ethanol (B)

Raman spectroscopy of FeS particles obtained via evaporation of water and ethanol reveals similar features (Fig. 3). For both spectra sharp peaks positioned at 250 and 310 cm^{-1} followed by less intensive broader peak at 420 cm^{-1} and broad peaks at 600 and 645 cm^{-1} have been detected. The peaks at 310 and 250 cm^{-1} are assignable to mackinawite ($Fe_{1+x}S$) phase [eg. 31, http://rruff.info reference R070302]. For mackinawite phase is typical also peak situated around 370 – 380 cm^{-1} [31] which could be demonstrated by less intensive peak at 370 (Fig. 3 A) and 377 cm^{-1} (Fig. 3 B). The broad peaks positioned at 600 and 645 cm^{-1} corresponds with the peaks of pyrhotite ($Fe_{1-x}S$) [31] and in accordance with the reference R060388 in the RRUFF database these peaks coincident also with mackinawite phase. In agreement with the reference R060440 spectrum (RRUFF database) peak at 420 cm^{-1} can be attributed to pyrhotite phase. The absence of bands at 206 and 280 cm^{-1}, which are characteristic for amorphous or weakly crystalline FeS phase [31], shows highly crystalline structure. In summary, Raman spectroscopy suggests formation of two-phase structure composed of mackinawite and pyrhotite phases. The phase transition from mackinawite into pyrrhotite is line with experimental data in aqueous solution [eg.32].

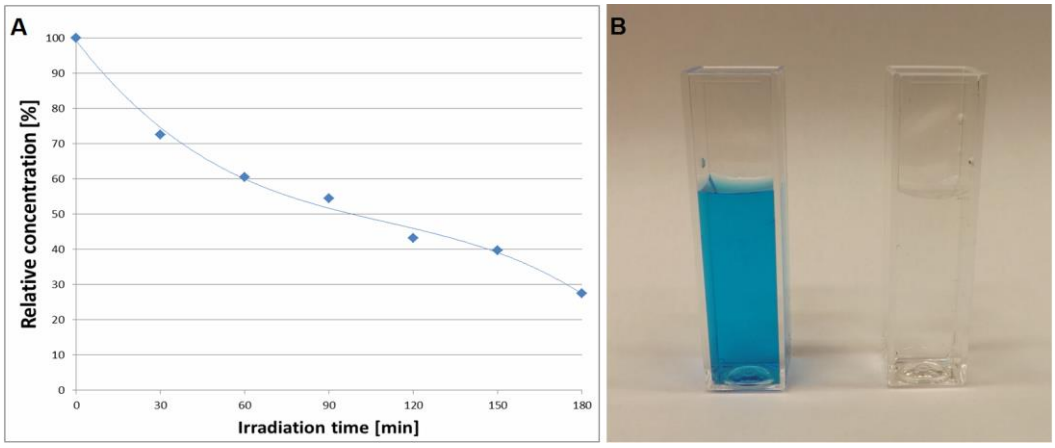

Fig. 4 Progress of MB degradation on light by FeS particles (A), photo of aqueous colloid before and after irradiation (180 min) at Φ ~ 800 lm of luminous flux.

The photocatalytic effect of aqueous FeS colloid was tested in terms of MB degradation. The mixture of 1ml of 0.05mM solution of MB and 2.5 ml of FeS aqueous colloid was exposed on daylight and the depletion of MB was measured by UV spectroscopy. Fig. 4 A shows significant MB degradation proceeding under daylight irradiation (without any external light source). After 180 minutes of irradiation ~27 % of original MB concentration remains. Fig. 4 B illustrates the image of the cuvettes with the mixture before (blue one) and after 180 minutes of daylight exposure (transparent one).

4. Conclusion

Laser ablation of FeS traget in the water and ethanol results in laser ablation and formation of nanoparticles and their clusters. Different colloid stability has been revealed for FeS colloid in water and ethanol. Size distribution of 100, 1000 and 5000 nm of particles in water together with the value of zeta potential 13.2 mV suggest tendency for agglomeration and incipient stability. In ethanol, one size of particles around 180 nm and the value of zeta -40.6 mV have been detected. It confirms good stability of this colloid. The morphology of obtained FeS particles was measured after evaporation of the liquids on Ta substrate. Shapeless, roundshape and sheet-like agglomerates of microparticles and spherical nanoparticles were shown by SEM. EDX revealed Fe/S ratio ~3.25 for particles obtained in water and ~ 1.2 for particles ablated in ethanol. Two-phase structure consisting of mackinawite ($Fe_{1+x}S$) and pyrrhotite ($Fe_{1-x}S$) was assigned by Raman spectroscopy. The photocatalytic activity of aqueous FeS colloid was tested by MB degradation under the daylight exposure.

Acknowledgements

The result was developed within the CENTEM project, reg. no. CZ.1.05/2.1.00/03.0088, cofunded by the ERDF as part of the Ministry of Education, Youth and SportsOPRDI programme and, in the follow up sustainability stage, supported through CENTEM PLUS (LO1402) by financial means from the Ministry of Education, Youth and Sports under the National Sustainability Programme I. Computational resources were provided by MetaCentrum (LM2010005) and CERIT-SC (CZ.1.05/3.2.00/08.0144) infrastructures.

References

[1] Hofmann W K, Birkholz M 1990 *Sol. Energy Mater* **20** 149
[2] Lehner S W, Savage K S, Ayers J S 2006 *J. Cryst. Growth* **286** 306
[3] Takahashi T 1973 *Solid State Commun.* **13** (9) 1335
[4] Wang H, Bigham J M, Tuovinen O H 2007 *Hydrometallurgy* **88** 127
[5] Bhar S K, Sumanta Jana S, Anup Mondal A, Nillohit Mukherjee N 2013 *Journal of Colloid and Interface Science* **393** 286 https://doi.org/10.1016/j.jcis.2012.10.049
[6] Villalba M, Peron J, Giraud M, Tard C 2018 *Electrochemistry communications* **91** 10 https://doi.org/10.1016/j.elecom.2018.04.019

[7] Sun Y, Lv D, Zhou J, Zhou X, Lou Z, Baig S A, Xu X 2017 *Chemosphere* **185** 452 https://doi.org/10.1016/j.chemosphere.2017.07.047
[8] Borah D, Senapati K 1999 *Nurs. Case Manag. Manag. Process Patient Care* **4** 85
[9] Bostick B C, Fendorf S 2003 *Geochim. Cosmochim*. **67** 909
[10] Bostick B C, Fendorf S, Helz G R 2003 *Environ. Sci. Technol.* **37** 285
[11] Doyle C S, Kendelewicz T, Bostick B C, Gordon Jr E B 2004 *Geochim. Cosmochim.* **68** 4287
[12] Soon J M, Goh L Y, Loh K P 2007 *Appl. Phys. Lett.* **91** 084105
[13] Vaughan D J, Lennie A R 1991 The iron sulphide minerals: their chemistry and role in nature, *Sci. Prog.* **75** 371 (Edinburgh)
[14] Rao C N R, Pisharody K P R 1975 *Prog. Solid State Chem.* **10** 207
[15] Goodenough J B 1978 *Mater. Res. Bull.* **13** 1305
[16] Bessergenev V 2004 *J. Phys. Condens. Matter* **16** S531
[17] Gosselin J R, Townsend M G,Tremblay R J 1976 *Solid Stat. Commun.* **19** 799
[18] Nakazawa H, Morimoto N 1971 *Mater. Res. Bull.* **6** 345
[19] Horwood J L, Townsend M G, Webster A H 1976 *J. Solid State Chem.* **17** 35
[20] Barnad A S, Russo S P 2007 *J. Phys. Chem.* **111** (31) 11742
[21] Almond M J, Redman H, Rice D A 2002 *J. Mater. Chem.* **10** 2842
[22] Ma X, Xu F, Wang X, Du Y, Chen L, Zhang Z 2005 *J. Cryst. Growth* **277** 314
[23] Chin P, Ding J, Yi J B, Liu B H 2005 *J. Alloys Compd*. **390** 255
[24] Morales-Gallardo M V, Ayala A M, Pal M, Cortes Jacome M A, Toledo Antonio J A, Mathews N R 2016 *Chemical Physics Letters* **660** 93 https://doi.org/10.1016/j.cplett.2016.07.046
[25] Pola J, Urbanová M, Pokorná D, Bezdička P, Kupčík J, Křenek T 2014 *RSC Adv*. **4** 11543 https://doi.org/10.1039/C3RA46580B
[26] Křenek T, Medlín R, Karatodorov S, Mihailov V, Pola M, Reshak A H 2017 *Journal of Alloys and Compounds* **723** 689 https://doi.org/10.1016/j.jallcom.2017.06.229
[27] Zeng H, Du X-W, Singh S C, Kulinich S A, Yang S, He J, Cai W 2012 *Adv. Funct. Mater*. **22** 1333 https://doi.org/10.1002/adfm.201102295
[28] Zhang Q, Yao X, Mwizerwa J P, Huang N, Wan H, Huang Z, Xu X 2018 *Solid State Ionics* **318** 60
[29] Wang X, Zhou W-H, Zhou Z-J, An Y-Q, Wu S-X 2013 *Materials Science in Semiconductor Processing* **16** 530
[30] Richard D, Luther G W 2007 *Chem. Rev.* **107** 514
[31] Mendili Y E, Abdelouas A, Hajj H E, Bardeau J-F 2013 *RSC Adv.* **3** 26343
[32] Rickard D T 1969 *Stockholm Contrib. Geol.* **26** 67